Praise Worthy Prize

International Review of Mechanical Engineering (I.RE.M.E.), Vol. 3, N. 1
January 2009

Investigation of Buckling of Steel Cylindrical Shells with Elliptical Cutout Under Bending Moment

Mahmoud Shariati, Masoud Mahdizadeh Rokhi

Abstract – *The cognition of the effect of cutout on the capacity of loading bearing and the buckling behavior of the cylindrical shells is crucial in designing of structures of automobiles, airplanes and marine structures. In this article, the simulation and analyzing of steel cylindrical shells with different lengths and diameters, including elliptical cutout, under bending moment with using of the numerical finite elements method was done. Furthermore, the effect of changing of cutout dimensions and the ratio of the length to diameter on buckling behavior and post buckling of cylindrical shells are studied. Finally, the relations for finding of buckling moment of these structures were presented.*

Keywords: *Buckling, Steel Cylindrical Shells, Elliptical Cutout, Bending Moment, Finite Element Method*

Nomenclature

L	Shell length
D	External Diameter
d	Internal Diameter
t	Shell thickness
a	Cutout height
b	Cutout width
M_{ref}	Reference moment
M	Buckling moment
E	Elasticity module
σ_y	Yield stress
Y	Poisson ratio
A	Cutout area
K	Correction factor
η	a/b ratio
γ	L/D ratio

I. Introduction

The cylindrical shells use in engineering structures such as airplanes, missiles, tanks, pipe lines, automobiles and submarine structures. These structures in their lifetime may be affected by buckling moments and buckle. The studies about this subject are very few. Yeh and Chen [1] examined the elastic bending buckling of a circular cylindrical shell with and without a cutout by the finite element method. Circular cylindrical shells under pure bending in the plastic range were also investigated. Kyriakides and Ju [2] and Ju and Kyriakides [3] investigated the instability of an aluminum cylindrical shell under pure bending with ratio of diameter to thickness in the range 19.5–60.5 and ratio of length to diameter in the range 18.1–30.1; they also observed the presence of wave-like ripples on the compression side of the bent tubes before collapse.

Shell buckling under combined bending and pressure was also examined [4], [5]. Corona and Kyriakides [4] found that the mode of collapse was correlated with the curvature of the cylindrical shell. Cyclic inelastic bending of tubes and the corresponding buckling problems were also reported [6]-[8]. When a cutout exists on a circular cylindrical shell, buckling usually occurs around the cutout. Yeu and his coworkers [9], fulfilled an experimental and analytical study about the bending buckling with cutout under pure bending.

They used the numerical method with a finite elements code with basis of the lagrangian formulizing and analyzed the bending buckling with regard to symmetry and nonlinear characteristics. In this study, the ratio of diameter to thickness for Aluminum specimens was 50 and the shape of cutout was considered as rectangular and circular. Furthermore, the effect of the length and location of cutout on bending moment was studied. Shu [10] obtained the plastic boundary loading for thin shell pipes with internal peripheral cracks under axial loading, internal pressure and asymmetrical bending moment.

Furthermore, he presented the formula for the combination of these loads. Li and Kettle [11], studied on bending response and buckling of ring-stiffened cylindrical shells under pure bending. They used a modified Brazier approach to investigate the nonlinear bending response of finite length cylindrical shells with stiffening rings. The nonlinear bending response was derived by applying the minimum potential energy principle and the corresponding critical moment associated with local buckling was determined by employing the Seide–Weingarten approximation. Elchalakani et al. [12] presented a plastic mechanism analysis for thin-walled circular hollow section tubes deforming in a multi-lobe collapse mode under large

Manuscript received and revised December 2008, accepted January 2009

deformation pure bending. An existing kinematic model for an axially compressed thin-walled circular tube modified to predict the collapse curve of a thin-walled tube under bending. Also an expression for the plastic collapse moment obtained by equating the total energy absorbed in bending, rolling and ovalisation to the external work carried out during a given cycle of deformation. Rahimi and Poor Saidi [13], studied the plastic strength of cylindrical shells with rectangular and circular cutouts under central, compression, bending and combining loading. They used the finite element method, PATRAN, and ABAQUS software.

They studied the different parameters such as shape, number and the length of cutout and the effect of reinforcement of around of the cutout. Vartdal et al. [14], considered the response of tubes with rectangular cut-outs to pure bending.

They tested Tubes containing cut-outs with an axial dimension of up to 30 mm and a circumferential size of up to 1808.

They found that plastic hinge mechanisms dominated the response when the cut-out was on the compressive side, whereas fracture behavior dominated the response when the cut-out was on the tensile side.

They carried out Finite element and semi-empirical analyses to predict the global load–deformation behavior of the tubes. Mathon and Limam [15], tested a large amount of thin shells (550<R/t<1450) of moderate length (L/R≈2) under internal pressure and pure bending loading.

They showed that one must distinguish between local buckling and global collapse of the structure. They compared their experimental data to design recommendations given by two standards (NASA SP8007 and Eurocode 3).

Shariati and Mahdizadeh [16], studied the effect of the position of elliptical cutouts with identical dimensions on the buckling and post-buckling behavior of cylindrical shells.

The shells with different diameters and lengths were studied.

Additionally, several buckling tests were performed using an INSTRON 8802 servo hydraulic machine, and the results were compared with the results of the finite element method.

In this article, we try to analyze the collection of linear and nonlinear analyses with using ABAQUS finite element software.

Our aim from these analyzes is the study of the effect of changing of dimensions of elliptical cutouts with constant area on the behavior of the buckling and post buckling of cylindrical shells with different lengths and diameters:

$$(L/D_1) = 2.857,\ 6.5,\ 10,$$

$$(L/D_2) = 2.495,\ 5.676,\ 8.732,$$

$$(D_1/t) = 53.846, (D_2/t) = 61.667$$

Furthermore, we presented the relations for finding of the buckling moment of these structures with using of the Lagrangian polynomial method.

II. Geometry and Mechanical Properties of the Shells

For this study, thin-walled cylindrical shells with three different lengths ($L = 120\,\text{mm}$, $273\,\text{mm}$, $420\,\text{mm}$), and two different diameters ($D = 42\,\text{mm}$, $48.1\,\text{mm}$) were analyzed.

An elliptical geometry was selected for cutouts that were created in the specimens.

Furthermore, the thickness of shells was $t = 0.78\,\text{mm}$.

Fig. 1 shows the geometry of the elliptical cutouts.

According to this figure, parameter (a) shows the size of the cutout along the longitudinal axis of the cylinder, and parameter (b) shows the size of the cutout in circumferential direction of the cylinder.

The distance between the center of the cutout and the lower edge of the shell is designated by L0, as shown in Fig. 1.

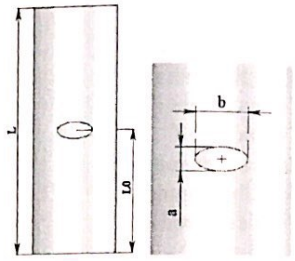

Fig. 1. Geometry of cutout

Specimens were nominated as follows:

$$D42 - L120 - L_0 60 - a - b$$

The numbers following D and L show the diameter and length of the specimen, respectively.

The cylindrical shells used for this study were made of mild steel alloy.

The mechanical properties of this steel alloy were determined according to ASTM E8 standard [17], using the INSTRON 8802 servo hydraulic machine.

The stress-strain curves, stress-plastic strain curve and respective values are shown in Figs. 2.

Based on the linear portion of stress-strain curve, the modulus of elasticity was computed as $E = 187.737\,\text{GPa}$ and the value of yield stress was obtained as $\sigma_y = 211\,\text{MPa}$.

Furthermore, the value of Poisson ratio was assumed $\nu = 0.33$.

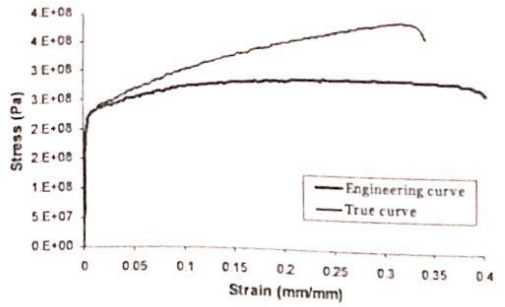

Fig. 2(a)

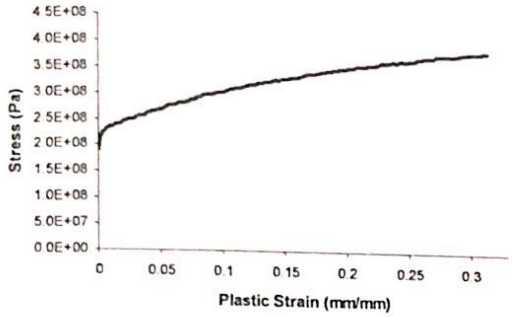

Fig. 2(b)

True strain	True stress (MPa)	Plastic strain	True stress (MPa)
0	0.000	0.00000	191.073
6.58e-5	25.280	0.00135	211.506
0.00023	63.010	0.00499	227.057
0.00045	106.830	0.01431	239.110
0.00066	150.620	0.02255	246.513
0.00084	175.980	0.03360	254.419
0.00104	191.07	0.04085	261.920
0.00247	211.506	0.05478	271.512
0.01225	235.136	0.06092	276.249
0.02386	246.513	0.07385	284.217
0.03496	254.419	0.08302	293.382
0.04488	263.261	0.09838	301.780
0.05622	271.512	0.10874	306.844
0.06729	280.063	0.12052	314.189
0.07536	284.217	0.13241	320.089
0.08872	296.220	0.14318	325.627
0.09999	301.781	0.15914	331.566
0.11279	309.086	0.18551	345.820
0.12660	316.361	0.19533	349.007
0.13874	322.896	0.20636	354.279
0.15396	328.374	0.21914	358.231
0.16895	335.947	0.23106	362.571
0.18456	343.195	0.24248	365.636
0.19961	349.866	0.26052	372.000
0.21384	355.697	0.27117	377.394
0.22749	360.545	0.28148	378.330
0.23999	365.326	0.29873	383.024
0.25811	370.322	0.30904	386.024
0.27509	377.857	0.31060	386.491
0.29851	383.657	0.31208	387.571
0.31556	387.465	0.31350	387.465

Figs. 2. (a) Stress – strain curves (b) Stress - plastic strain curve (For more information about true stress-strain curve and plastic property refer to [18], ABAQUS analysis user's manual, part IV, section 11.1.1) and respective values (Over 150 data were obtained from tensile test; therefore some of them were shown here

III. Loading and Boundary Conditions

The shells are modeled as "two ends clamped" and the bending moment is applied to two rigid planes, attached to two margins of shell.

Furthermore, the shells are applied under bending moment in three directions; bending toward of cutout, toward the opposite side of cutout and in the plane parallel to cutout (Figs. 3).

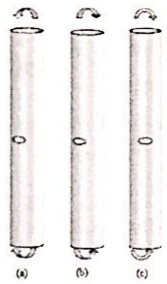

Figs. 3. Directions of applied bending moments to specimens: (a)Bending toward of cutout, (b) The opposite side of cutout, (c) In the plate parallel to cutout

All of the freedom degrees of two shells edges are limited, except for longitudinal moving and rotation along the moment applying.

IV. Element Formulation of the Specimens

For meshing of specimens the nonlinear element S8R5 (that is an eight node with six freedom degrees for each node and is suitable for thin shells analyzing) was used.[18]. A meshed specimen was shown in Fig. 4.

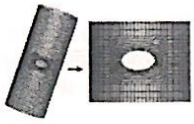

Fig. 4. A sample of FEM mesh

V. Analytical Process

Eigenvalue analysis, overestimates the value of buckling load, because in this analysis the plastic properties of material do not have any role in analyze procedure. For buckling analysis, an eigenvalue analysis should be done initially for all specimens, to find the mode shapes and corresponding eigenvalues. Primary modes have smaller eigenvalues and buckling usually occurs in these mode shapes. For eigenvalues analysis the "Buckle" step was used in software. Three initial mode shapes and corresponding displacements of all specimens was obtained. The effects of these mode shapes must be considered in nonlinear buckling analysis

(Static Riks step). Otherwise, the software would choose the buckling mode in an arbitrary manner, resulting in unrealistic results in nonlinear analyze. For "Buckle" step, the Subspace solver method of the software was used. It is noteworthy that due to the presence of contact constraints between rigid plates and the shell, the Lanczos solver method cannot be used for these specimens [18]. In Figs. 5, three primary mode shapes are shown for the specimen D42-L120-$L_0$60-8-17.7 .

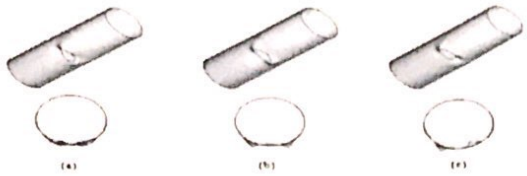

Figs. 5. Buckling mode shapes for specimen D42-L120-$L_0$60-8-18: (a) first mode, (b) second mode, (c) third mode

After completion of the Buckle analysis, a nonlinear analysis was performed to plot the load-displacement curve. The maximum value in this curve is the buckling load. This step is called "Static Riks" and uses the arc length method for post-buckling analysis. In this analysis, nonlinearity of material properties and geometry are both taken into consideration.

VI. The Reference Cylindrical Shell

For drawing of diagrams, it is better that the data became no dimension. For this purpose, we defined the reference moment for specimens as following:

$$M_{ref} = \frac{\pi\sigma_y\left(D^4 - d^4\right)}{32D} \qquad (1)$$

In this relation, M_{ref} is the reference moment that is the necessary moment for the yielding cylindrical shells. D and d are the external and internal diameters of cylinders, respectively. σ_y is the yield stress of the material of the specimens. Thus, the reference moment for specimens obtains as following:

$$M_{ref} = \frac{212\pi\cdot 10^6\ N/m^2\left(0.042m^4 - 0.0404m^4\right)}{32\cdot 0.042m} = 216.646Nm \quad for \quad D = 42mm \qquad (2)$$

$$M_{ref} = \frac{212\pi\cdot 10^6\ N/m^2\left(0.048m^4 - 0.0465m^4\right)}{32\cdot 0.0481m} = 286.172Nm \quad for \quad D = 48.1mm \qquad (3)$$

VII. Results of Numerical Analyzing

In this section, the results of numerical analyzing of cylindrical shells with elliptical cutout and constant area, under bending moment, is presented. For this purpose, a cutout with approximate area of $A = 111.2mm^2$ was considered and four values for the height of cutout between extents of 8-17.7mm were selected and the related width was obtained.

Three different shell lengths were analyzed, representing short (L=120mm), intermediate-length (L=273mm) and long cylindrical shells (L=420mm).

VII.I Applying of the Moment Toward the Cutout

The results of analyses are presented in the Table I.

TABLE I
SUMMARY OF NUMERICAL ANALYSIS FOR CYLINDRICAL SHELLS WITH ELLIPTICAL CUTOUT UNDER MOMENT TOWARD THE CUTOUT

Model designation	Shell length (mm)	Cutout size $(a\times b)$ $(mm\times mm)$	Buckling Moment (N.m)
D42 – L420 – Perfect	420	-----	297.646
D42 – L420 – $L_0$210 – 8 – 17.7	420	8 × 17.7	188.674
D42 – L420 – $L_0$210 – 11 – 12.87	420	11 × 12.87	203.249
D42 – L420 – $L_0$210 – 14 – 10.11	420	14 × 10.11	211.026
D42 – L420 – $L_0$210 – 17.7 – 8	420	17.7 × 8	216.773
D42 – L273 – Perfect	273	-----	297.891
D42 – L273 – $L_0$136.5 – 8 – 17.7	273	8 × 17.7	189.28
D42 – L273 – $L_0$136.5 – 11 – 12.87	273	11 × 12.87	204.143
D42 – L273 – $L_0$136.5 – 14 – 10.11	273	14 × 10.11	212.012
D42 – L273 – $L_0$136.5 – 17.7 – 8	273	17.7 × 8	215.683
D42 – L120 – Perfect	120	-----	297.157
D42 – L120 – $L_0$60 – 8 – 17.7	120	8 × 17.7	200.732
D42 – L120 – $L_0$60 – 11 – 12.87	120	11 × 12.87	214.494
D42 – L120 – $L_0$60 – 14 – 10.11	120	14 × 10.11	222.349
D42 – L120 – $L_0$60 – 17.7 – 8	120	17.7 × 8	227.255
D48.1 – L420 – Perfect	420	-----	385.329
D48.1 – L420 – $L_0$210 – 8 – 17.7	420	8 × 17.7	248.432
D48.1 – L420 – $L_0$210 – 11 – 12.87	420	11 × 12.87	264.185
D48.1 – L420 – $L_0$210 – 14 – 10.11	420	14 × 10.11	271.742
D48.1 – L420 – $L_0$210 – 17.7 – 8	420	17.7 × 8	277.77
D48.1 – L273 – Perfect	273	-----	385.13
D48.1 – L273 – $L_0$136.5 – 8 – 17.7	273	8 × 17.7	248.19
D48.1 – L273 – $L_0$136.5 – 11 – 12.87	273	11 × 12.87	265.995
D48.1 – L273 – $L_0$136.5 – 14 – 10.11	273	14 × 10.11	273.145
D48.1 – L273 – $L_0$136.5 – 17.7 – 8	273	17.7 × 8	278.064
D48.1 – L120 – Perfect	120	-----	399.861
D48.1 – L120 – $L_0$60 – 8 – 17.7	120	8 × 17.7	263.802
D48.1 – L120 – $L_0$60 – 11 – 12.87	120	11 × 12.87	286.812
D48.1 – L120 – $L_0$60 – 14 – 10.11	120	14 × 10.11	294.165
D48.1 – L120 – $L_0$60 – 17.7 – 8	120	17.7 × 8	299.222

Considering of these results, it is obvious that with creating of the cutout in shell, the buckling moment decreases, greatly. For example with creating of a cutout with dimensions of $8 \cdot 17.7mm$ in the shell with $L/D = 10$ and $D/t = 53.846$ ratios, the buckling moment decreases about 37 percent.

In Fig. 6, the buckling moment with respect to the L/D ratio is shown.

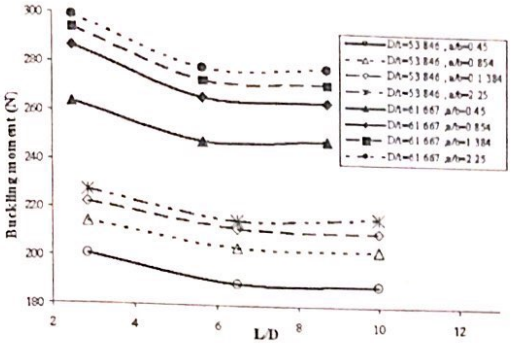

Fig. 6. Summary of the buckling moment vs. L/D ratio for cylindrical shells include elliptical cutout with constant area

We consider that for L/D<6 ratios, the buckling moment decreases with increasing the L/D ratio, but the buckling moment is constant for 6<L/D<10 ratios. Furthermore, the shells with greater diameters have the greater buckling moment.

The buckling moment curves in respect to the a/b ratio are shown in Fig. 7.

We consider that with increasing of the a/b ratio, the buckling moment increases. Furthermore, the shells with greater diameters are more resistance against buckling.

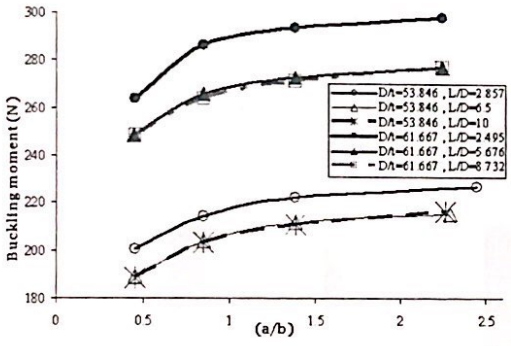

Fig. 7. Summary of the buckling moment vs. a/b ratio for cylindrical shells include elliptical cutout with constant area

The curves of moment, angular displacement of the end edges are shown in Figs. 8. We consider that the shells with the greater a/b ratios are higher from other curves. In addition, we see that with creating a cutout in specimens, the great changes in treatment of buckling moment curve in respect to the end rotation is resulted.

With comparing of the curves in Figs. 8, we can result that the slopes of curves of the specimens without cutout are a little greater than the specimens with cutouts. Furthermore, the slopes of the curves of the specimens with cutouts and greater width are greater than the specimens with cutouts and less width that shows the decreasing of specimen's stiffness in pre buckling part with creating of the cutout and increasing of the width of cutout. The Von misses stress contours for two specimens with L/D=6.5 and D/t=53.846 ratios are shown in Figs. 9 and 10. We see in these figures that before reaching of the moment to critical amount, the stress in almost of the shell area (unless for the area around the cutout) distributes regularly and increases with increasing of moment. The stress contours for specimens with cutout are symmetric, completely.

In the areas around the cutout, the stress concentration and amount of it increases. (Figs. 9(a)) and 10(a)) and the area of these areas toward the shell periphery increases and finally the shell buckles. We consider from Figs. 9 that the buckling under bending moment is both local and global, because in time of buckling, the shells edges have rotated about 0.003 radiant. Furthermore, with comparing of stress contours in specimens in Figs. 9 and 10, it is obvious that with increasing of a/b ratio, the distribution of stress in the side with cutout, unless of around of cutout, is more regular. In addition, the area of surrounded area in buckling state increases that means (with regard to the cutout symmetry) the increasing of stress or applying moment on shell.

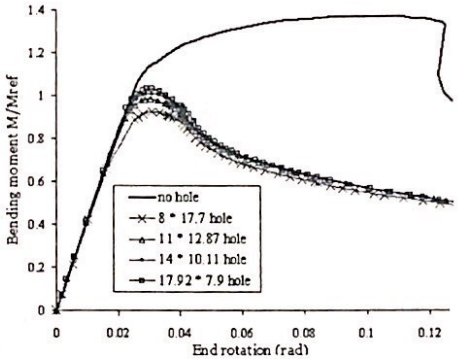

Fig. 8(a). L/D=10 and D/t=53.846

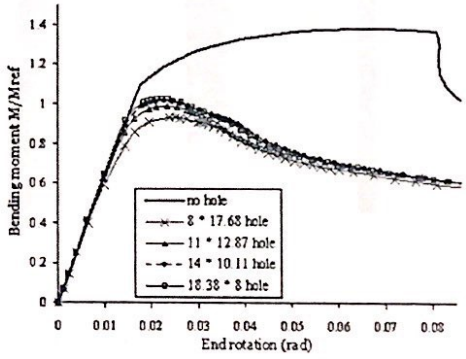

Fig. 8(b). L/D=6.5 and D/t=53.846

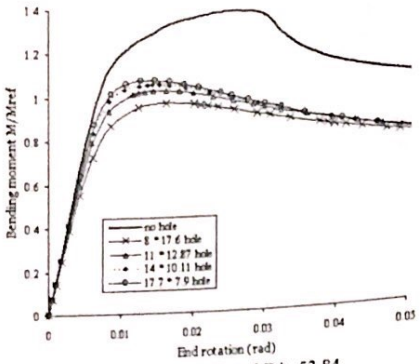

Fig. 8(c). L/D=2.857 and D/t=53.84

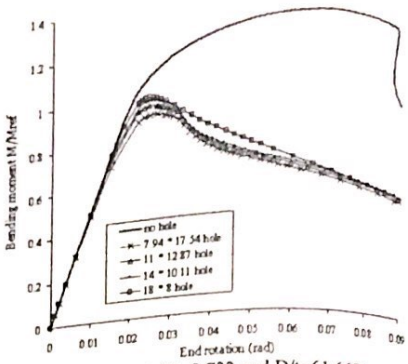

Fig. 8(d). L/D=8.732 and D/t=61.667

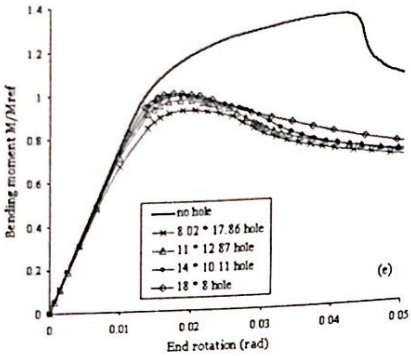

Fig. 8(e). L/D=5.676 and D/t=61.667

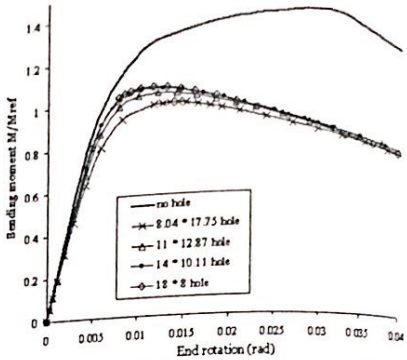

Fig. 8(f). L/D=2.495 and D/t=61.667

Figs. 8. Bending moment - end rotation, behavior of cylindrical shells with and without an elliptical cutout with constant area

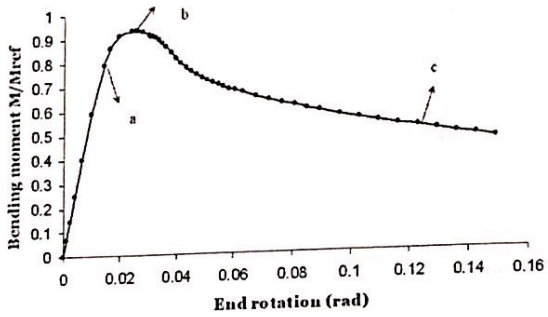

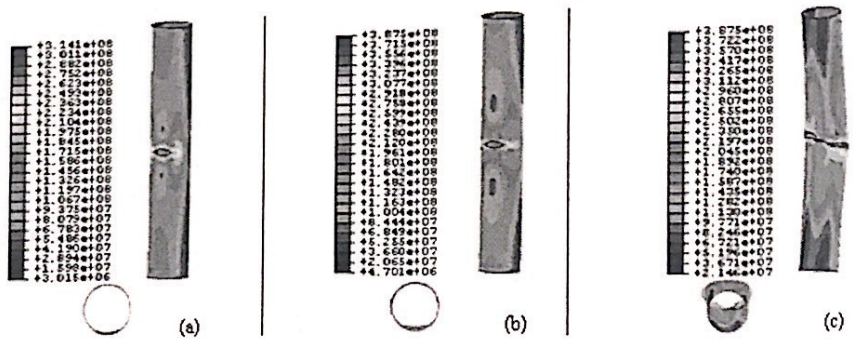

Figs. 9. Plots of bending moment vs. end rotation, the shell deformations and von mises stress states contours at various loading stages of the specimen D42-L273-$L_0$136.5-8-17.68

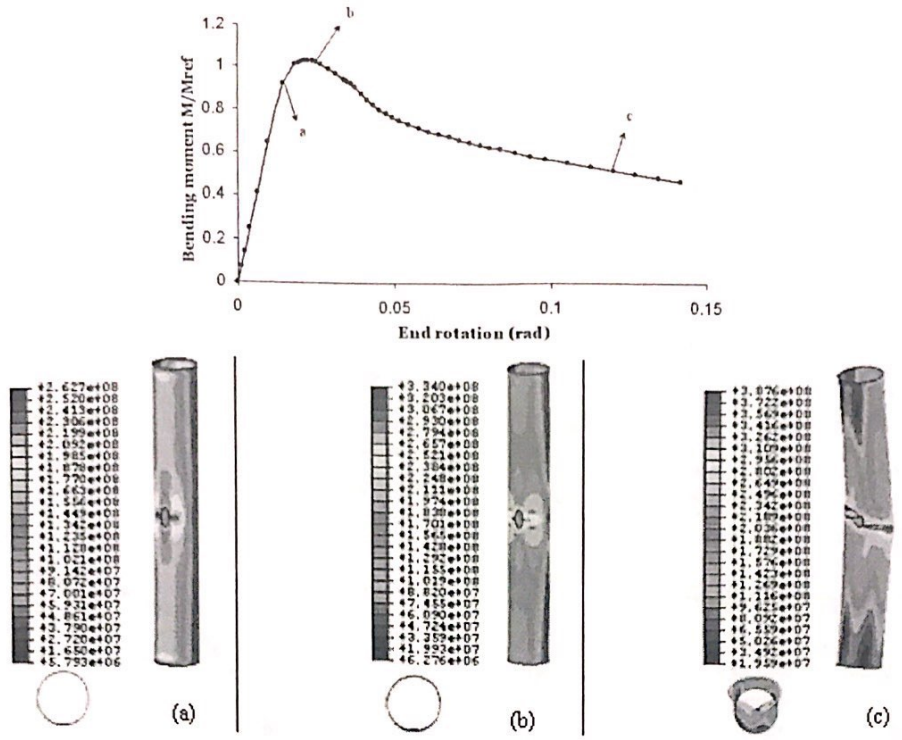

Figs. 10. Plots of bending moment vs. end rotation, the shell deformations and von mises stress states contours at various loading stages of the specimen D42-L273-$L_0$136.5-18.38-8

VII.2 Applying of Moment Toward the Opposite Side of Cutout

Table II shows the results of some cylindrical shells with average length and D/t=53.846 ratio, under moment toward the opposite side of cutout.

TABLE II
SUMMARY OF NUMERICAL ANALYSIS FOR CYLINDRICAL SHELLS WITH ELLIPTICAL CUTOUT UNDER MOMENT TOWARD THE OPPOSITE SIDE OF CUTOUT

Model designation	Shell length (mm)	Cutout size ($a \times b$) ($mm \times mm$)	Buckling Moment (N.m)
$D42-L273-L_0136.5-8-17.7$	273	8×17.7	282.116
$D42-L273-L_0136.5-11-12.87$	273	11×12.87	290.699
$D42-L273-L_0136.5-14-10.11$	273	14×10.11	293.46
$D42-L273-L_0136.5-17.7-8$	273	17.7×8	294.692

From comparing of these results with previous results, we result that the shell resistance against buckling in the case of applying of moment toward the opposite side of cutout is greater than the case that moment applies toward the cutout.

Furthermore, similar to the previous case, we consider that with increasing of the cutout width the buckling moment decreases and vise versa.

VII.3. Applying the Moment in the Plate Parallel to Cutout

Table III shows the results of analyzing of some cylindrical shells with average length and D/t=53.846, under moment in the plane parallel to cutout.

TABLE III
SUMMARY OF NUMERICAL ANALYSIS FOR CYLINDRICAL SHELLS WITH ELLIPTICAL CUTOUT UNDER MOMENT IN THE PLATE PARALLEL TO CUTOUT

Model designation	Shell length (mm)	Cutout size ($a \times b$) ($mm \times mm$)	Buckling Moment (N.m)
$D42-L273-L_0136.5-8-17.7$	273	17.7×8	286.789
$D42-L273-L_0136.5-11-12.87$	273	12.87×11	291.99
$D42-L273-L_0136.5-14-10.11$	273	10.11×14	293.745
$D42-L273-L_0136.5-17.7-8$	273	8×17.7	296.774

From comparing of these results with the previous results, we concludes that the resistance of shell against buckling is greater than two previous cases, if the moment applies Figs. 11 shows the specimen $D42-L273-L_0136.5-8-17.7$ at the time of buckling and under moment in three different directions.

We consider that the buckling is local if the moment applies toward the cutout, but with applying of moment

toward the opposite side of cutout or applying of moment in the plane parallel to cutout, the global buckling occurs.

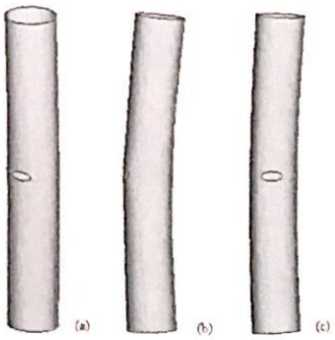

Figs. 11 Deformation of specimen in buckling state: (a) Direction of moment toward the cutout, (b) Direction of moment toward the opposite side of cutout, (c) Direction of moment in the plate parallel to cutout

VIII. Numerical Relations

In this section, we present the relations for computing of buckling moment of cylindrical shells with elliptical cutout, under bending moment toward the cutout, with using of the Lagrangian polynomial [19] and the numerical results. For using of these relations, the buckling moment of cylindrical shells without cutout must be known. The K_{cutout} coefficient defines as following:

$$K_{cutout} = \frac{M_{cutout}}{M_{perfect}} \tag{4}$$

In this relation, $M_{perfect}$ is the buckling moment of the shells without cutout, M_{cutout} and K_{cutout} are the buckling moment and the correction coefficient for the shells with cutout, respectively. K_{cutout} is computed with assistance of the Lagrangian polynomial. The obtained relations are as following:

$$\begin{aligned} K_{Cutout} &= 0.02504\eta^3 + 0.2276\eta \\ &+0.0018\gamma^2 + 0.01604\gamma\eta + 0.0007\gamma\eta^3 \\ &-0.0082\gamma\eta^2 + 0.00038\gamma^2\eta^2 - 0.001\gamma^2\eta \\ &+0.655 - 0.1226\eta^2 - 0.0305\gamma - 0.00001\gamma^2\eta^3 \end{aligned} \tag{5}$$

$$\begin{aligned} K_{Cutout} &= -0.0078\gamma + 0.001\gamma^2 \\ &+0.00033\gamma^2\eta^3 + 0.00022\gamma^2\eta^2 - 0.001\gamma^2\eta \\ &-0.0078\gamma\eta^3 + 0.0134\gamma\eta^2 - 0.0089\gamma\eta \\ &+0.5337 + 0.07747\eta^3 + 0.4547\eta - 0.3113\eta^2 \end{aligned} \tag{6}$$

That $\eta = a/b$ and $\gamma = L/D$.

The relation 5 presents the correction coefficient of buckling moment for cylindrical shells with $D/t = 53.846$ ratio and different length $2.857 \le L/D \le 10$ with elliptical cutout and constant area $A = 111.2mm^2$ and different dimensions ($0.45 \le a/b \le 2.22$) in the middle of shell. The relation 6 presents the correction coefficient of buckling moment for cylindrical shells with $D/t = 61.667$ ratio and different length $2.4948 \le L/D \le 8.732$ with elliptical cutout and constant area $A = 111.2mm^2$ and different dimensions ($0.45 \le a/b \le 2.22$) in the middle of shell.

The fitting functions in Eqs. (5) and (6) are the equations of surfaces that pass through the data obtained by simulations. Figs. 12 and 13 represent a section of these surfaces for $\gamma = 10$ that pass through the FEM results exactly.

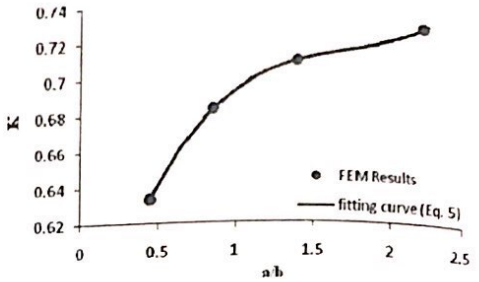

Fig. 12. Plots of data obtained by simulations and the Lagrange polynomial (Eq. 5) for shells with D/t=53.846 and γ=10

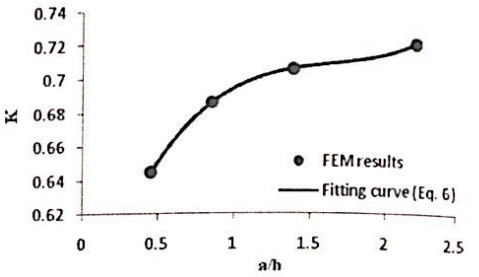

Fig. 13. Plots of data obtained by simulations and the Lagrange polynomial (Eq. 6) for shells with D/t=61.667 and γ=10

IX. Conclusion

With creating of cutout in shell, the buckling moment of shell decreases greatly. With increasing the L/D ratio, the buckling moment decreases. In addition, increasing the shell diameter for a constant thickness leads to increasing of buckling moment. With increasing the ratio of the height to width of elliptical cutout (a/b) the buckling moment, increases.

Creating of cutout in shell and increasing the width of cutout lead to decreasing of the shell stiffness before buckling. When moment applies toward the cutouts, the buckling moment is less than the case that moment

applies toward the opposite side of cutout or in the plane parallel to cutout. Finally, we obtained the coefficients for getting the buckling moment of cylindrical shells with elliptical cutout from the buckling moment of complete shells.

References

[1] M. K. Yeh, J. Chen, Bending buckling of thin circular cylinders, *Proc. 15th National Conference on Theoretical and Applied Mechanics*, Taiwan, ROC, 1991, pp. 729–35 (in Chinese).

[2] S. Kyriakides, G. T. Ju, Bifurcation and localization instabilities in cylindrical shells under bending, I. Experiments. *Int. J. Solids Struct. Vol. 29*, pp. 1117–42, 1992.

[3] G.T. Ju, S. Kyriakides, Bifurcation and localization instabilities in cylindrical shells under bending II. Predictions. *Int. J. Solids Struct. Vol. 29*, pp. 1143–71, 1992.

[4] E. Corona, S. Kyriakides, An unusual mode of collapse of tubes under combined bending and pressure, *ASME J. Press. Vessel Technol. Vol. 109*, pp. 302–4, 1987.

[5] E. Corona, S. Kyriakides, On the collapse of inelastic tubes under combined bending and pressure, *Int. J. Solids Struct, Vol. 24*, pp. 505–35, 1988.

[6] S. Toma, WF. Che, Cyclic inelastic analysis of tubular column sections, *Comput. Struct, Vol. 16*, pp. 707–16, 1983.

[7] Pk. Shaw, S. Kyriakides, Inelastic analysis of thin-walled tubes under cyclic bending, *Int. J. Solids Struct, Vol. 21*, pp. 1073–100, 1985.

[8] PK. Shaw, S. Kyriakides, Inelastic buckling of tubes under cyclic bending, *ASME J. Press. Vessel. Technol, Vol. 109*, pp. 169–78, 1987.

[9] MK. Yeh, MC. Lin, WT. Wu, Bending buckling of an elastoplastic cylindrical shell with a cutout, *Eng. Struct, Vol. 21*, pp. 996–1005, 1999.

[10] S. Hengmu, The Plastic Limit Load of Circumferentially Cracked Thin Walled Pipes under Axial Force, Internal Pressure and Asymmetrical Bending, *Int. J. Press. Vesssel Piping, Vol. 79*, pp. 377-382, 2002.

[11] L. Li, R. Kettle, Nonlinear bending response and buckling of ring-stiffened cylindrical shells under pure bending. *Int. J. of Solids and Struc, Vol. 39*, pp. 765–781, 2002.

[12] M. Elchalakani, R. Grzebieta, X. Zhao, Plastic Collapse Analysis of Slender Circular Tubes Subjected to Large Deformation Pure Bending, *Advances in Structural Eng., Vol. 5, n. 4*, pp. 241-257, 2002.

[13] G. H. Rahimi sh., E. poursaeedi, Parametric study of plastic strength of cylindrical shells with cutout under axial loading and bending moment, *J. of mech. Eng., Iranian society of mechanical engineers. 6th year, Vol. 1*, pp. 504-512, 2004.

[14] B. J. Vartdal, S. T. S. Al-Hassani, S. J. Burley, A tube with a rectangular cut-out. Part I: subject to pure bending. *Proc. IMechE, Part. C: J. Mechanical Engineering Science, Vol. 220(C5)*, 2006, pp. 625–643.

[15] C. Mathon, A. Limam, Experimental collapse of thin cylindrical shells submitted to internal pressure and pure bending, *Thin-Walled Structures, Vol. 44*, pp. 39–50, 2006.

[16] M. Shariati, M. Mahdizadeh R., Numerical and Experimental Investigations on Buckling of Steel Cylindrical Shells with Elliptical Cutout Subject to Axial Compression, *Thin-Walled Structures. Vol. 46*, pp. 1251– 1261, 2008.

[17] Standard Test Methods and Definitions for Mechanical Testing of Steel Products (ASTM A 370 – 05).

[18] ABAQUS 6.4-PR11 user's manual.

[19] C. F. Gerald, P. O. Wheatley, Applied Numerical Analysis, . Addison Wesley, New York, 1999.

Authors' information

Department of Mechanical Engineering,
Shahrood University of Technology,
Daneshgah Boulevard, Shahrood, Iran.

E-mail:mshariati@shahroodut.ac.ir

M.Shariati has born in Mashhad city, the second biggest city of IRAN at 1966.

He is an associate professor in mechanical engineering (applied mechanics) in Shahrood university of technology, Shahrood town, Semnan province. His interest scientific fields are "*fatigue and fracture mechanics, stress analysis and applied design of structures and machines*" He has published over 50 papers at journals and conferences until now. Also he has two inventions about design and fabrication of microtunnelling machines. He has done over ten research plan. He has guide over ten Ms.C and Ph.D. students at this time. Dr Shariati take his Ph.D. degree in mechanical engineering from Tarbiat Modares University at 1999, Tehran.

M. Mahdizadeh Rokhi has born in Mashhad city of IRAN at 1982.

He is a Ph.D student of Mechanical Engineering (Applied Design) in Shahrood University of Technology, Shahrood city, Iran. His major fields of study are "*fatigue and fracture mechanics, shells and plates, nano mechanics.*"He has published 5 papers at journals and conferences with cooperation of Dr. Shariati until now.Mr. Mahdizadeh is member of Elite National Institute of IRAN.